EAI Endorsed Transactions
on Scalable Information Systems
Research Article EAI.EU

Virtual reality simulation research on the quality and strength of the riveting process for the top cover accessory of battery pack

Wang Yang-qing[1,*]; Tang Wenke[1]; Ning Shui-gen[1]; Cao Bing-xin[1]

[1]Jiujiang Vocational and Technical College, Jiujiang 332007, Jiang Xi, China

Abstract

INTRODUCTION: Based on the riveting theory, a 3D model of the riveting structure was established, and the riveting process of three kinds of plate thickness was simulated by Deform-3D virtual simulation, and the theoretical values of the key parameters of the riveting structure were obtained.
OBJECTIVES: Through the tensile and shear tests of riveted samples, it was found that the simulation theory of key parameters of riveting was close to the experimental values, which showed the feasibility of the simulation.
METHODS: Through the experiment, it was further found that the shear strength and tensile strength were increased with the increase of plate thickness.
RESULTS: The shear strength and tensile strength of a 1.5mm thick plate were increased by 81.2% and 35.2%, respectively, compared with that of a 1.0mm thick plate. The shear resistance and tensile strength of the 2.0 mm thick plate were 111.4% and 54.5% higher than that of the 1.0 mm thick plate.
CONCLUSION: During the experiment, it was not found that the upper and lower plates were separated directly, but the neck of the riveted joint was directly broken.

Keywords: Battery Pack; Top Cover; Riveting without rivets; Virtual reality, Deform-3D, Rivet Less joint strength.

Received on 09 08 2024, accepted on 05 02 2025, published on 12 02 2025

doi: 10.4108/eetsis.6865

1. Introduction

As a kind of plastic forming joint process, rivet less surface damage, stable connection quality and other significant advantages, have been widely used in the automotive field and aviation field [1,2]. In electric vehicles, this process is mainly applied in the connection of components, and the riveting without rivets connection is widely used in the connection of the battery pack structure [1]. The battery pack sealing top cover is generally made of plastic steel or aluminium alloy, but the use of thin aluminium alloy greatly reduces the weight of the battery pack to a certain extent, there are certain difficulties in the installation of the top cover accessories. The top accessories are mostly used for fixing wiring harnesses, cooling water pipes and other functions (as shown in the structural relationship in Figure 1. The wiring harness and cooling water pipe are fixed on the top cover by spot welding or self-tapping screws. Due to the thin thickness of the top cover, the top cover will be destroyed by spot welding at high temperatures and self-tapping screw mode. Because the riveting without rivets process belongs to cold stamping, it is relatively friendly to the deformation and damage of the top cover, and the connection process has small surface damage and simple process, and has been widely used in the fixing of attachments [2,3]. There is a problem of

*Corresponding author. Email: 1401490318@qq.com, wang_yanqin48@outlook.com

limited mechanical strength of joints in riveting without rivets [4]. In this paper, 5754 aluminium alloy plates are taken as the research object, according to the geometric parameters of the joint, the simulation model is established, and the connection strength and bearing capacity of the riveted joint under load are deeply studied by the combination of simulation and experiment.

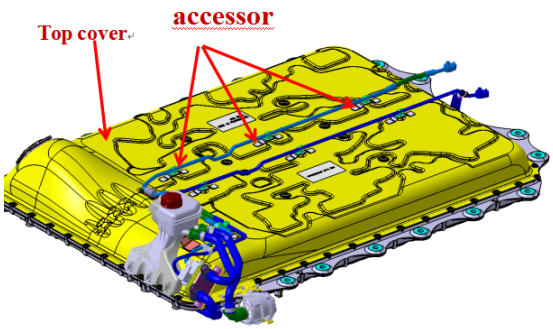

Figure 1. Structure relationship of the top cover

2. Theoretical strength and evaluation of riveting without rivets process

2.1. Riveting without riveting process

The riveting joint is a method of cold stamping, which uses the die to cold press the upper and lower plates, and the plastic deformation of the plates makes the plates deformed and embedded in the mould to achieve the connection [4]. In the riveting connection process, the plate is mainly extruded by the punch, and the material is inlaid in the die. The riveting process is shown in Figure 2. The two layers of sheet metal are extruded by the punch down into the die during the initial pressing of sheet metal. The upper plate has a large shear deformation and becomes thinner under the extrusion of the punch, while the lower plate has a relatively small deformation. In the early stage of forming, the punch continues to move downward, and the upper plate is deformed and thinned to flow into the bottom groove of the die, but the lower plate has not entered the inside of the die. In the forming stage, the punch continues to go down, the lower plate flows to the concave die under a strong extrusion pressure and gradually fills the inside of the concave die, and the upper plate is gradually embedded into the lower plate of the concave die under a strong extrusion pressure, thus producing a joint point between the upper and lower plates.

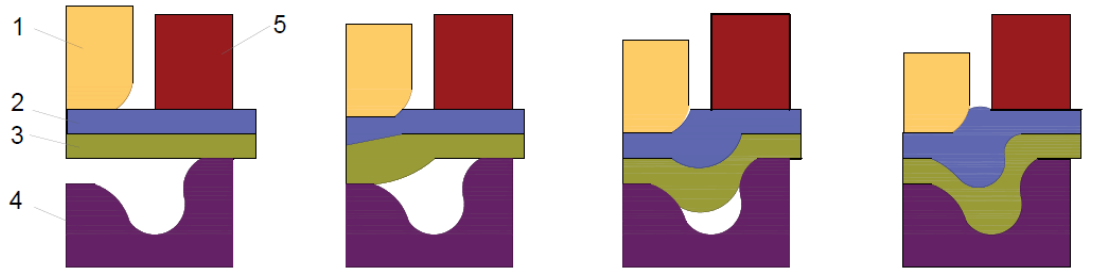

Figure 2. Riveting without rivets process

2.2. Quality evaluation of riveted joints without rivets

The quality of riveting without rivets can be evaluated by observing the joint and testing the mechanical properties of the joint [5]. Observation of riveted joints is a common intuitive evaluation method. The joint strength is evaluated by measuring the structural parameter values of the riveted joint. The geometric structure of the joint centre section is shown in Figure 3, and its geometric parameters include neck thickness value T_n, interlock value T_u and bottom thickness value X. The quality of riveting without rivets is evaluated by observing the change in joint structural parameters. According to the literature [6], the riveting strength is directly

affected by neck thickness value, interlocking value and bottom thickness value. The smaller the neck thickness value, the easier the joint is to break. The interlock value is related to the stability and reliability of the joint. The larger the interlock value is, the more reliable the joint connection is.

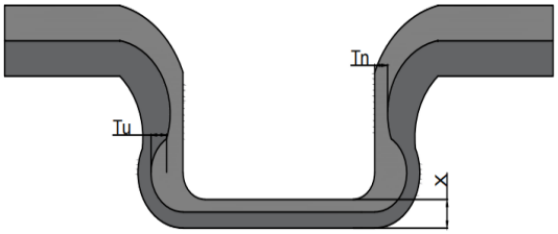

Figure 3. Geometric structure and parameters of riveting without rivets joint centre section

2.3. Joint strength and failure form

According to the literature [6-8], the main failure loads of riveting without rivets joints are tensile and shear, respectively. In this paper, the axial tensile and transverse shear tests of riveted plates of different thicknesses will be conducted to explore the tensile strength, shear strength and the factors affecting the strength of riveting without rivets joints.

2.3.1. Theoretical calculation of shear strength of the joint

Figure 4-a shows the transverse shear force applied to the joint. When the transverse shear force gradually increases to a certain value, the neck of the connector will be shear fractured, as shown in Figure 4-b. At this time, when the joint reaches the yield limit, a neck shear fracture occurs, and the maximum shear force F_1 is estimated as follows [6]:

$$F_1 = \tau_s \pi \left[\left(\frac{d}{2} + T_n \right)^2 - \left(\frac{d}{2} \right)^2 \right] \quad (1)$$

Where: τ_s is the shear strength of the plate;d is the diameter of the riveted punch; T_n is the neck thickness.

From the formula analysis, it can be seen that when the plate and riveting die are selected, the shear strength of the plate and the punch diameter are fixed, and the maximum shear force F_1 is proportional to the neck thickness T_n.

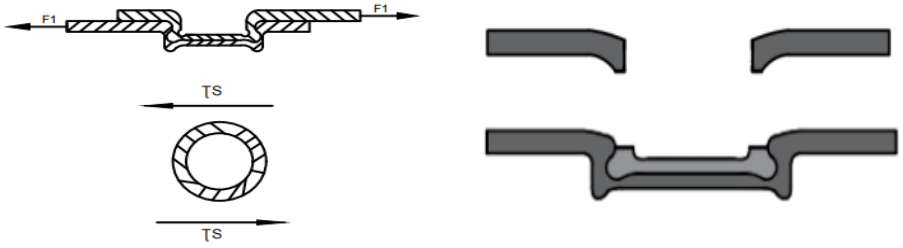

（a）Shear force diagram （b） Neck fracture failure mode

Figure 4. Schematic diagram of transverse shear force

2.3.2. Theoretical calculation of joint tensile strength

The riveted joint is subjected to axial tension, resulting in two modes of separation, namely neck fracture and upper and lower plate detachment, as shown in Figure 5. The formula for calculating the tensile force F_2 when a neck fracture occurs is as follows [6]:

$$F_2 = R_{p0.2} \pi \left[\left(\frac{1}{2} d + T_n \right)^2 - \left(\frac{d}{2} \right)^2 \right] \quad (2)$$

Where: $R_{0.2p}$ is the tensile yield strength of the plate.

The maximum axial tensile load F_3 for the failure of the upper plate and the lower plate is calculated as follows [6]:

$$F_3 = \frac{\pi}{4} \left[(d + 2T_n)^2 - d^2 \right] R_{0.2p} \frac{\tan\theta + f}{f} \bullet \left\{ 1 - \left[\frac{T_n (d + T_n)}{(T_n + T_u)(T_u + T_u + d)} \right] \frac{f}{\tan\theta} \right\} \quad (3)$$

Where: f is the friction factor between the upper and lower plates, and θ is the embedding Angle.

It can be seen from the analysis of these formulas that TOX connection strength is positively correlated with neck thickness, interlock value embedding Angle, etc. The greater the connection strength is, the better the connection process quality is.

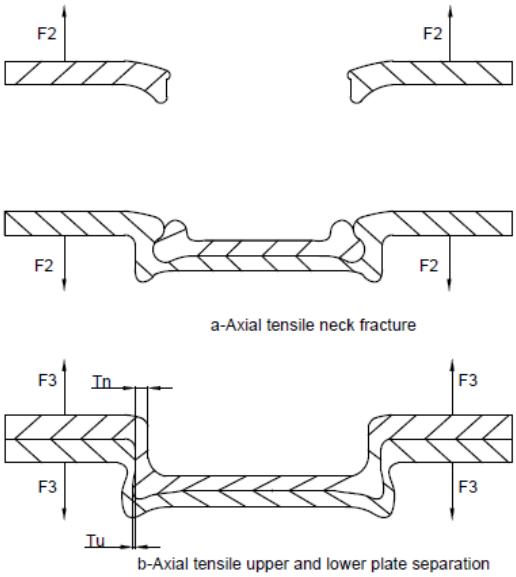

Figure 5. Schematic diagram of axial tensile force

3. Simulation and analysis of the riveting process without rivets

3.1. Simulation model establishment and pre-processing

In this paper, the AL5754 thin plate was used for riveting without riveting. AL5754 aluminium alloy is an excellent choice for the riveting process due to its well-balanced mechanical properties, including moderate strength, corrosion resistance, and weldability. With a yield strength of approximately 98.3 MPa and a tensile strength of around 227.2 MPa, it provides the durability needed for joints subjected to significant stress. The magnesium content enhances its corrosion resistance, making it particularly suitable for demanding environments such as marine and automotive applications, where longevity and reliability are critical. Additionally, AL5754's high ductility allows for significant plastic deformation without cracking, ensuring secure interlocking during the riveting process. Its lightweight nature contributes to overall weight reduction, which is essential for industries prioritizing fuel efficiency and performance. Moreover, the alloy's good thermal conductivity helps dissipate heat generated during riveting, preserving joint integrity.

The properties of this material are as follows: the elastic model is 70Gpa, the yield strength is 98.3MPa, the tensile strength is 227.2MPa, the elongation is not less than 18%, and the density is 2.79g/cm3. Deform-3D software was used to conduct virtual simulation, and a riveting without rivets simulation model of plates with thicknesses of 1.0mm, 1.5mm and 2.0mm was established. The simulation model is shown in Figure 6. In the simulation, the upper and lower plates are set as plastic bodies, and the moulds are set as rigid bodies [9-11]. The friction coefficient between the upper and lower plates, the punch (upper punch) the upper plate and the holder ring and the upper plate is 0.2, the friction coefficient between the lower plate and the die is 0.3, and the stamping speed is 5mm/s. The simulation model sets the upper punch diameter to d=5.4mm, the upper punch rounded Angle R to 0.5mm, the lower die diameter D to 8.0mm, the depth of the die H to 1.4mm, and the radius of the lower die groove to 0.5mm.

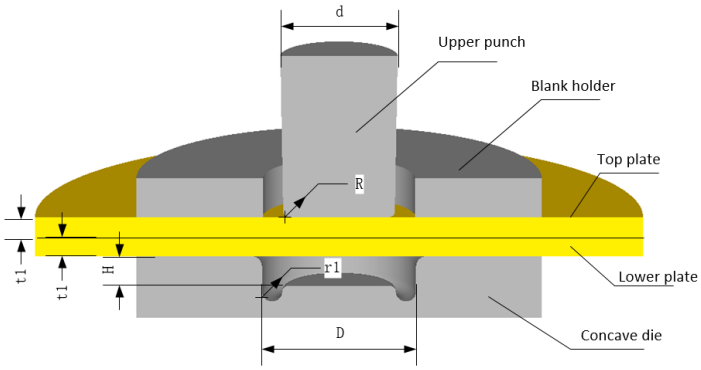

Figure. 6. Simulation model diagram

3.2. Simulation Results

In the research, riveting simulation research was carried out on three kinds of plates with equal thickness of 1.0mm, 1.5mm and 2.0mm, and the equivalent strain distribution cloud map of the sections of the three plates after riveting without rivets was obtained, as shown in Figure 7. From the simulated cloud image, it can be found that the stress concentration in the contact neck area and the interlocking area of the plates with three thicknesses occurs, and the material flows to the inside of the die under extrusion. In the simulation results, three quality evaluation parameters, neck thickness T_n, interlock T_u and bottom thickness X, were measured, and the data obtained are shown in Table 1. The simulation data in Table 1 was substituted into formula (1) - (3) to estimate the tensile force and shear force. The results are shown in Table 2.

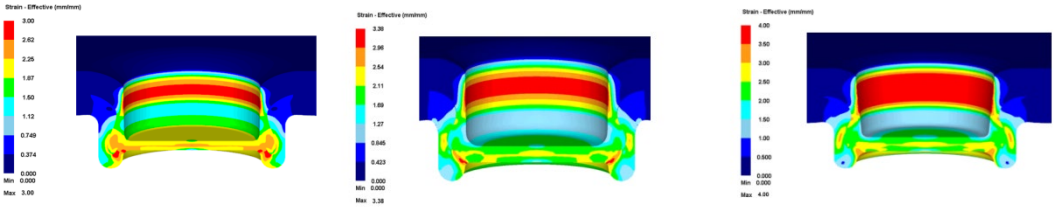

a 1.0mm b 1.5mm c 2.0mm

Figure 7. Equivalent strain cloud diagram of the joint of plates with different thicknesses

Table 1. The average values of neck thickness, interlock value and bottom thickness obtained from simulation results

Thickness（mm）	Neck thickness value (mm)	Interlock value (mm)	Bottom thickness value (mm)
1.0	0.295	0.343	0.48
1.5	0.346	0.357	0.75
2.0	0.463	0.401	0.82

Table 2. Theoretical tensile and shear resistance of riveted joints

Thickness（mm）	F_1(N)	F_2(N)	F_3(N)
1.0	518.55	1198.54	1199.07
1.5	613.66	1418.96	1419.58
2.0	870.71	2013.33	2014.21

4. Test analysis

4.1. Test Preparation

The riveting test setting was consistent with the simulation parameters. Three groups of sheet materials of 1.0mm,1.5mm and 2.0mm were prepared according to the test requirements, and the size of sheet material was 25mm×80mm. The shear and tensile samples are shown in Figure 8.

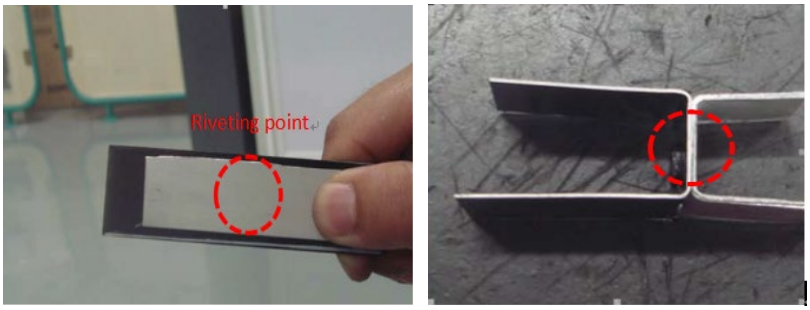

a. Transverse shear test samples b. Axial tensile test samples

Figure 8. Test sample

4.2. Riveting test

The riveting experiment without rivets was completed on the test machine, as shown in Figure 9. In the test, the test sample is placed on the lower concave die, the upper die moves downward gradually with the push of the testing machine, and the upper and lower plates are pressed into the concave die due to extrusion pressure, thus forming a riveting point. The riveted samples of 3 specifications were selected and cut along the centre line of the samples respectively, and the parameters of the riveted joints were detected by a video measuring instrument [12]. The video measurement images are shown in Figure 10. The neck thickness, interlock value and bottom thickness value of the riveted structure were measured, and the data comparison was shown in Table 3 and Figure 11. In the data comparison chart, it is found that the experimental values of neck thickness, interlock value and bottom thickness value are all lower than the theoretical simulation values. The error of neck thickness value in the 1.0mm plate thickness group is 1.35%, the error of interlock value is 9.01%, and the error of bottom thickness value is 10.4%. The error of neck thickness in the 1.5mm plate thickness group is 6.64%, the error of interlock value is 5.04%, and the error of base thickness value is 9.33%. The error of neck thickness value in the 2.0mm plate thickness group is 4.75%, the error of interlock value is 4.48%, and the error of base thickness value is 7.3%.

From the data analysis, it can be seen that the experimental values are close to the simulation theoretical values, indicating that the simulation theoretical calculation is credible, and the subsequent simulation research on tensile and shear resistance is of credible value.

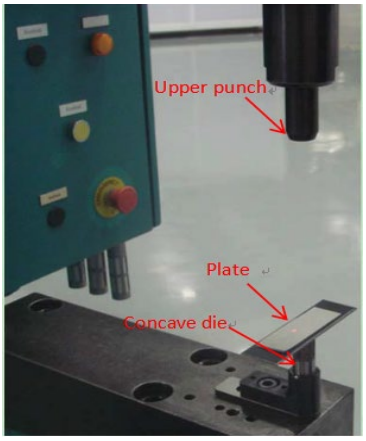

Figure 9. Riveting experimental device

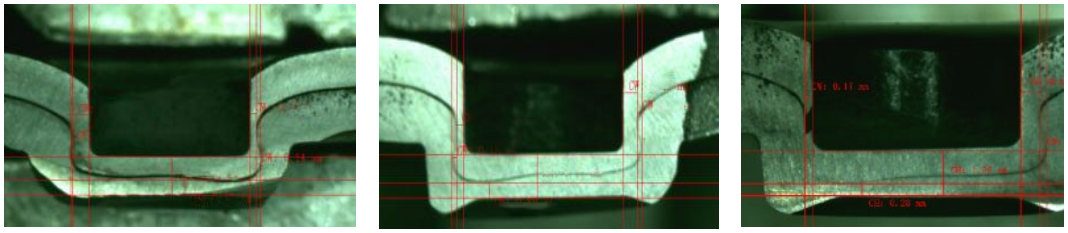

a 1.0mm b1.5mm c 2.0mm

Figure 10. Cutting diagram of the joint of plates of different thickness

Table 3. Comparison between simulation value and test value

Plate Thickness (mm)	Neck Thickness (mm) (Simulated)	Neck Thickness (mm) (Tested)	Bottom Thickness (mm) (Simulated)	Bottom Thickness (mm) (Tested)	Interlock Value (mm) (Simulated)	Interlock Value (mm) (Tested)
1	0.295	0.291	0.48	0.43	0.343	0.312
1.5	0.346	0.323	0.75	0.68	0.357	0.339
2	0.463	0.441	0.82	0.76	0.401	0.383

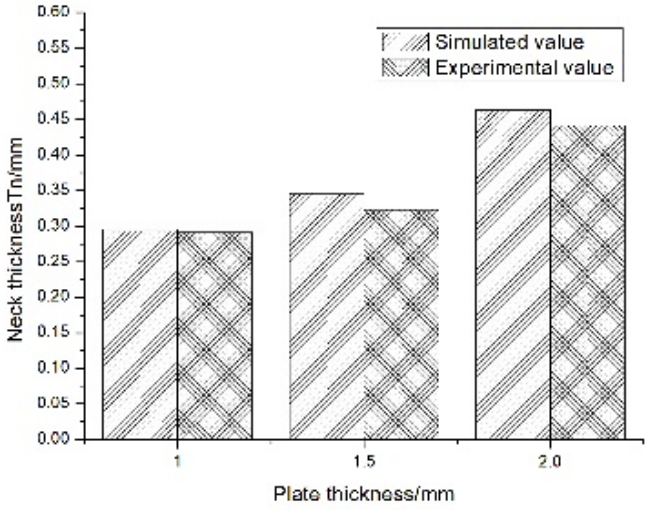

(a) neck thickness value

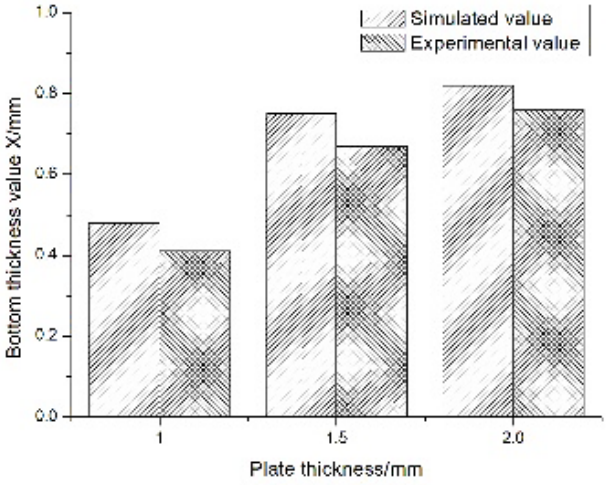

(b) bottom thickness value

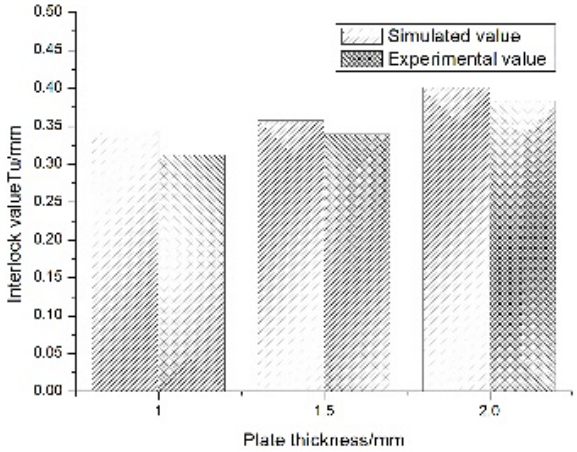

(c) interlock value

Figure 11. Comparison between simulation value and test value

4.3. Mechanical Test

Tensile and shear tests are carried out on the mechanical testing device to further verify whether the theoretical calculation of tensile and shear forces is reasonable. The test process is shown in Figure 12. In the test, the tensile and shear tests of three samples with different thickness specifications were carried out, each test was carried out 3 times, and the average tensile and shear forces were calculated. During the test, it was found that the riveted neck was broken, but no neck detachment was found. The failure forms of tensile and shear resistance are shown in Figure 13.

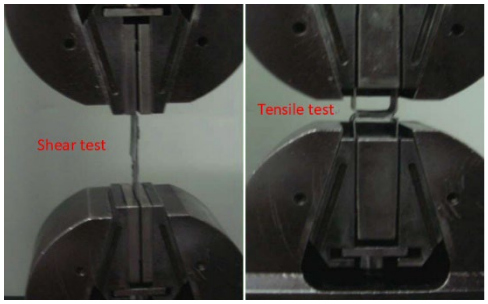

Figure 12. The test site

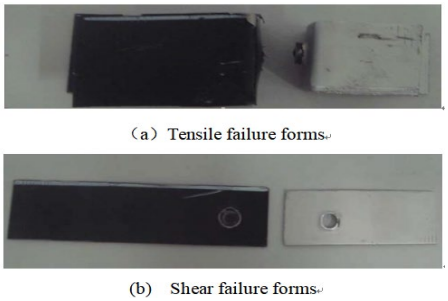

Figure 13. The failure forms of tensile and shear

In the process of mechanical testing, it was found that the shear strength and tensile strength increased with the increase of plate thickness. The shear resistance and tensile strength of the 1.5mm thick plate were increased by 81.2% and 35.2% respectively, compared with that of the 1.0mm thick plate. The shear resistance and tensile strength of the 2.0mm thick plate were increased by 111.4% and 54.5% respectively, compared with that of the 1.0mm thick plate. The data results are shown in Table 4 and Figure 14. In the mechanical test, it was not found that the upper and lower plates were separated, but the neck was broken. The tensile force and shear force obtained by the mechanical test became more obvious with the increase in plate thickness, and both were greater than the theoretical value, which was due to the problem of the value of the theoretical yield limit. The mechanical test ends with the separation between the two plates, and the plates have reached the breaking limit when separated, so there was no direct separation between the upper and lower plates.

Table 4. Comparison of the results of shear force and tensile force

Plate thickness/mm	Shear force/N		Tensile force/N	
	Simulated value	Experimental value	Simulated value	Experimental value
1	510	525	1200	1210
1.5	600	920	1400	1650
2.0	860	1100	2000	2250

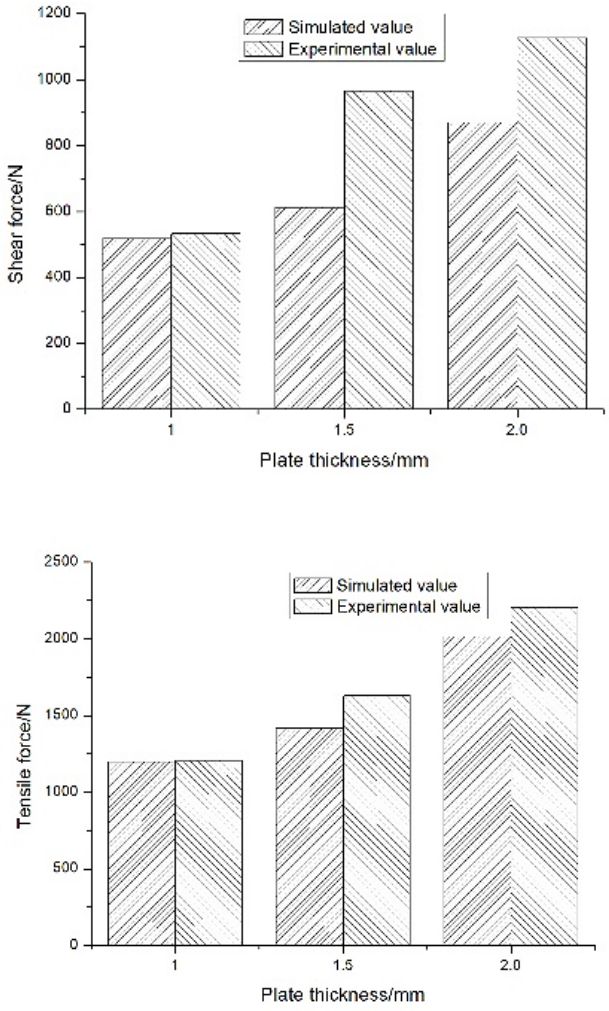

Figure 14. Comparison of the results of shear force and tensile force

5. Discussion

The Deform-3D simulation of the riveting process is based on plastic forming theory, modelling material deformation under pressure to create strong mechanical interlocks. The process involves localized plastic deformation as a punch presses two overlapping sheets into a die, generating compression and shear forces that enhance joint strength. Friction plays a significant role in material flow and shear stress distribution, with coefficients set to simulate real-world conditions. The simulation parameters include a punch diameter of 5.4 mm, a punch rounded edge of 0.5 mm, a die cavity diameter of 8.0 mm, and a die cavity depth of 1.4 mm, all of which influence joint formation and strength. Shear and tensile loading conditions were modelled using theoretical equations, showing that neck thickness (T_n) significantly impacts joint resistance to failure. The study employed the Finite Element Method (FEM) for stress-strain analysis, considering nonlinear plasticity models and strain rate sensitivity. Equivalent strain and stress distribution cloud maps identified areas of high deformation concentration, validating theoretical predictions. Comparisons between simulation and experimental data showed close agreement, with an error margin of 1.35% to 10.4%, confirming model accuracy. Further, experimental findings indicated that increasing plate thickness improved shear and tensile strength, with failures occurring primarily through neck fractures rather than plate separation. Ultimately, the study demonstrated that Finite Element Modeling (FEM) effectively predicts mechanical properties in riveting processes, reinforcing the importance of plastic deformation mechanics in improving joint reliability and performance.

5.1. Practical Implications

The proposed virtual reality (VR) simulation model for evaluating the quality and strength of the riveting process has broad practical applications across multiple industries. In the automotive sector, it enhances the assembly of lightweight aluminium battery packs in electric vehicles (EVs), ensuring structural integrity while preventing thermal damage caused by welding. It also optimizes riveting in car body manufacturing, improving crash safety and lightweight design. In the aerospace industry, the model aids in designing durable riveted joints for aircraft panels, optimizing material usage, and reducing experimental costs. Similarly, manufacturing and industrial engineering benefit from the model by improving sheet metal fabrication, predicting failure points, and ensuring better quality control. The renewable energy sector utilizes it in energy storage system designs, ensuring reliable connections in solar and wind power storage units. Additionally, the model serves as a VR-based training tool, helping engineers and technicians refine riveting techniques in a risk-free environment. It is also valuable in consumer electronics for ensuring durable connections in lightweight casings for laptops and smartphones, as well as in construction for secure modular aluminium structures. The defence industry benefits from its application in military-grade equipment, improving durability under extreme conditions. Overall, the model enhances production efficiency, reduces material waste, and accelerates prototype development by allowing manufacturers to simulate and optimize riveting parameters before full-scale production.

6. Conclusion

(1) The neck thickness, interlock value and bottom thickness obtained by simulation theory are slightly higher than the experimental value obtained by the riveting test. The error between the theoretical neck thickness and the experimental value is 1.35%-6.64%, the error between the theoretical interlock value and the experimental value is 4.48%-9.01%, and the error between the theoretical bottom thickness and the experimental value is 7.3%-10.4%, indicating that the simulation calculation method was correct and credible value.
(2) The shear resistance and tensile strength were increased with the increase of plate thickness, 1.5mm thick plate compared with 1.0mm thickness plate, the shear resistance and tensile strength increased by 81.2% and 35.2% respectively; The shear resistance and tensile strength of 2.0mm thick plate were 111.4% and 54.5% higher than that of 1.0mm thickness plate.
(3) The tensile force and shear force obtained by the experiment increase with the increase of plate thickness, and both are greater than the theoretical value, which is due to the value of the theoretical yield limit.
(4) At the end of the experiment, no direct separation of the upper and lower plates was found, but a direct fracture of the neck was found. The reason is that at the end of the experiment, the experimental value of the tensile force is much higher than the theoretical value F_3, which leads to the fracture of the neck structure.

The proposed model for riveting battery pack structures has several limitations, including a discrepancy between simulation results and experimental findings, higher tensile and shear forces in experimental tensile and shear forces than theoretical values, and an inability to account for all possible failure mechanisms. The study focused solely on AL5754 aluminium alloy, which may limit applicability to other

materials. Additionally, process variables like friction, punching speed, and tool wear were fixed in the simulations, which can vary in real-world applications. To improve the model's accuracy and practicality, future research should include expanding the study to include different aluminium alloys or composite materials, optimizing rivet geometry through modifications in punching processes, refining the simulation models with advanced material properties, strain-hardening effects, and failure criteria, investigating the long-term durability of riveted joints under thermal and mechanical stress, and integrating machine learning techniques to optimize riveting parameters. These improvements could lead to more accurate simulations and better-performing riveting techniques for battery pack structures.

Declarations

Funding

This research work was supported by the Science and Technology Project of the Jiangxi Education Department (GJJ2204802).

Conflict of interest

The authors declare that they do not have any commercial or associative interest that represents a conflict of interests in connection with the work submitted. Thanks to Wang Yang-qing for his contribution to the experimental testing work, and to Dr. Ning Shui-gen for his valuable suggestions in the research work.

Data Availability

All data generated or analysed during this study are included in the manuscript.

Code Availability

Not applicable.

Author's contributions

All authors contributed to the design and methodology of this study, the assessment of the outcomes and the writing of the manuscript.

References

[1] Ning S, Fu H, Tang W, et al. Virtual simulation stamping forming analysis and experiment of battery pack top cover. Comput Aided Des Appl. 2023;20(S14):93-101. DOI: 10.14733/cadaps.2023.S14.93-101.

[2] Weiliang Z, Baoyun Q, Hui W. Research on TOX riveting properties of dissimilar metals. In: Proc 5th Int Conf Mech Control Comput Eng (ICMCCE); 2020; Harbin, China. p. 498-501. DOI: 10.1109/ICMCCE51767.2020.00114.

[3] Vorderbrüggen J, Köhler D, Grüber B, Troschitz J, Gude M, Meschut G. Development of a rivet geometry for solid self-piercing riveting of thermally loaded CFRP-metal joints in automotive construction. Compos Struct. 2022; 291:115583. DOI: 10.1016/j.compstruct.2022.115583.

[4] The experimental analysis of forming and strength of clinch riveting sheet metal joints made of different materials. Adv Mech Eng. 2013;5. DOI: 10.1155/2013/848973.

[5] Mucha J, Kaščák Ľ, Witkowski W. Research on the influence of the AW 5754 aluminium alloy state condition and sheet arrangements with AW 6082 aluminium alloy on the forming process and strength of the clinch-rivet joints. Materials. 2021; 14:2980. DOI: 10.3390/ma14112980.

[6] Wang Y, Hou H, Chen X, et al. Analysis of rivet quality and strength of plate without rivet. J Plast Eng. 2022;29(3):93-100. (In Chinese). DOI: 10.3969/j.issn.1007-2012.2022.03.013.

[7] Xu Z. Research on forming law and technology of rivet joint [Master's thesis]. Guilin, China: Guilin Univ Electron Technol; 2014. (In Chinese).

[8] Rusia A, Weihe S. Development of an end-to-end simulation process chain for prediction of self-piercing riveting joint geometry and strength. J Manuf Process. 2020; 57:519-532. DOI: 10.1016/j.jmapro.2020.07.004.

[9] Fang Y, Huang L, Zhan Z, et al. A framework for calibration of self-piercing riveting process simulation model. J Manuf Process. 2022; 76:223-235. DOI: 10.1016/j.jmapro.2022.01.015.

[10] Du Z, Duan L, Jing L, Cheng A, He Z. Numerical simulation and parametric study on the self-piercing riveting process of aluminium–steel hybrid sheets. Thin-Walled Struct. 2021; 164:107872. DOI: 10.1016/j.tws.2021.107872.

[11] Zhang X, Yu HP, Li CF. Multi-field coupling numerical simulation and experimental investigation in electromagnetic riveting. Int J Adv Manuf Technol. 2014; 73:1751-1763. DOI: 10.1007/s00170-014-5983-4.

[12] Hönsch F, Domitner J, Sommitsch C, Götzinger B, Kölz M. Numerical simulation and experimental validation of self-piercing riveting (SPR) of 6xxx aluminium alloys for automotive applications. J Phys Conf Ser. 2018; 1063:012081. DOI: 10.1088/1742-6596/1063/1/012081.